Supporting Information

Quadrangular prism-like oxidized tin sulfide for high activity CO_2ER to formate

Jingru Zhang,[a,b] Xi Hu,[a] Haidong Li,[a] Yanqiu Du,*[a] Zidong Wei,*[b] and Xuejie Liu*[a]

[a] College of Materials and Textile Engineering, Jiaxing University, Jiaxing 314001, China

[b] School of Chemistry and Chemical Engineering, Chongqing University, Chongqing, 400044, China

* Corresponding author: E-mail: xuejliu@zjxu.edu.cn

1. Experimental Section

Materials. Tin tetrachloride (IV) pentahydrate ($SnCl_4·5H_2O$, AR) was purchased from Boer chemical reagents. Zinc chloride ($ZnCl_2$, AR) was obtained from Macklin reagent. sodium hydroxide (NaOH, AR) and ethylene diamine tetraacetic acid (EDTA, AR) were supplied by Chongqing chuandong chemical. Thioacetamide (TAA, AR) was purchased from Shanghai Adamasi reagents. All reagents were used without further purification.

Preparation of zinc stannate ($ZnSn(OH)_6$) precursor. In a typical experiment, tin tetrachloride (IV) pentahydrate ($SnCl_4·5H_2O$) is used as the tin source, while zinc chloride ($ZnCl_2$) serves as the zinc source. Based on the Hard-Soft-Acid-Base theory, in the presence of borderline acid Zn^{2+}, it is difficult for hard acid Sn^{4+} to react with soft base S^{2-} to form SnS_2 due to strong binding affinity and coordination stability between Zn^{2+} and S^{2-}. However, in a hydrothermal experiment, Sn^{4+} can be allowed to react sufficiently with S^{2-} and synthesize SnS_2 and O-SnS_2 catalysts through introducing ethylene diamine tetraacetic acid (EDTA) to remove Zn^{2+}. According to the above research frame, the quadrangular prism-like zinc stannate ($ZnSn(OH)_6$) precursor is first prepared using a simple hydrothermal method[1].

The hydroxide precursor was prepared through a hydrothermal method. At room temperature, 0.50 g of $SnCl_4·5H_2O$ and 0.19 g of $ZnCl_2$ were added to a PTFE reaction vessel containing 20 mL of deionized water. The mixture was stirred to obtain a homogeneous solution. Then, 20 mL of 0.5 M NaOH solution was added to above solution and stirred until a white slurry is formed. Afterwards, the reaction vessel was transferred to a stainless steel autoclave and subjected to hydrothermal treatment at 130 °C for 20 hours. After the reaction, the vessel was naturally

cooled to room temperature, and the resulting product was separated by centrifugation and washed with deionized water at least three times. Finally, the purified product was dried in an oven, and the white powder obtained was the target $ZnSn(OH)_6$ precursor.

Preparation of $Sn_xZn_yO_z$ quadrangular prisim. The $Sn_xZn_yO_z$ quadrangular prisim was prepared through oxidizing the $ZnSn(OH)_6$ precursor in a muffle furnace at 600 °C for 2 hours. The muffle furnace was heated to 600 °C at a rate of 5 °C/min.

Synthesis of oxidized tin sulfide (O-SnS_2) quadrangular prism: O-SnS_2 quadrangular prism was obtained by sulfidation treatment of Zn_xSnyO_3 using a hydrothermal method. At room temperature, 85.8 mg of Zn_xSnyO_3, 135 mg of TAA and 240 mg of H_4EDTA were sequentially added to a PTFE reaction vessel containing 60 mL of deionized water under stirring. After complete dissolution, the reaction vessel was transferred to a stainless steel autoclave and subjected to hydrothermal reaction at 220 °C for 3 hours. Then, the vessel was naturally cooled to room temperature. The resulting product was separated by centrifugation and washed with deionized water repeatedly. Finally, the O-SnS_2 microcube was obtained by drying the purified product in an oven and the dried sample was yellow powder.

Synthesis of O-ZnS/SnO_2 quadrangular prism: O-ZnS/SnO_2 quadrangular prism was also prepared by hydrothermal method. 85.8 mg of Zn_xSnyO_3, 135 mg of TAA were sequentially added to a PTFE reaction vessel containing 60 mL of deionized water under stirring at room temperature. The subsequent synthesis and separation process were the same as the previous preparation of O-ZnS/SnO_2 microcubes.

Synthesis of tin sulfide (SnS_2) microflower. 85.8 mg of $ZnSn(OH)_6$, 135 mg of TAA and 240

mg of H_4EDTA were sequentially added to a PTFE reaction vessel containing 60 mL of deionized water under stirring at room temperature. The subsequent synthesis and separation process were the same as the previous preparation of O-SnS_2 quadrangular prism.

Density Functional Theory Calculations. All Density Functional Theory (DFT) computations were conducted using the Vienna Ab-initio Simulation Package (VASP) with the projector augmented-wave (PAW) method. In the modeling process, the surface thickness was set to 3, and a vacuum layer of 15 Å was included in the z-direction. The PAW method was employed to accurately represent ion-electron interactions. The Perdew-Burke-Ernzerhof (PBE) functional was utilized to describe electron-electron exchange and correlation effects. Additionally, onsite Coulomb interactions were incorporated to account for the localized d electrons of transition metals. For all DFT simulations, the cutoff energy for the plane wave basis was set to 500 eV, and the k-point density was configured to 3x3x1. The residual force for optimizing atomic positions was kept below 0.02 eV $Å^{-1}$. Using the crystal planes tested by HRTEM as the adsorption crystal planes of the catalyst, set the adsorption sites at the metal Sn sites. The absorption models for all intermediates were meticulously explored to ensure results that closely reflect realistic conditions.

2. Characterization

Scanning electron microscope (SEM) measurements were performed on a JEOL JSM-7800F. The SEM samples were prepared by dropping 10 μL of the sample ethanol solution on a clean silicon wafer, and then dried at room temperature. After 30 seconds of gold sputtering, place it in the sample chamber for testing. Transmission electron microscopy (TEM), scanning transmission

electron microscopy (STEM) and energy dispersive x-ray detector (EDX) elemental mapping measurement was characterized on Thermo Scientific Talos F200S at an accelerating voltage of 200 kV. 1 μL of the sample ethanol dispersion was deposited on carbon-coated copper grids, and samples were allowed to dry under atmosphere conditions. X-ray diffraction spectra were measured using a LabX XRD-6000. The radiation source is Cu Kα, with a diffraction angle range of 5° to 90° and a scan speed of $5°\cdot min^{-1}$. X-ray photoelectron spectroscopy was recorded by Thermo Scientific ESCALAB250Xi. BET analysis were conducted on BELSORP MAX II. A suitable amount of finely ground catalyst was added in pre-weighed empty tube, and dried at 120 °C for 12 hours before reweighing. Then, in a nitrogen environment, the surface of sample was cold with liquid nitrogen until physical adsorption equilibrium was achieved. Thermogravimetric analysis was conducted on SHIMADZU DTG-60H. The test temperature ranged from room temperature to 800°C, with a heating rate of $5°C\cdot min^{-1}$ in an N_2 atmosphere.

3. Electrochemical performance testing of catalysts

Preparation of the working electrode. 4 mg of catalyst was dispersed in 800 μL of ethanol solution, then adding 5 μL of 0.5 wt.% Nafion solution. Ultrasonicate for 1 hour to obtain a uniformly dispersed catalyst suspension. Subsequently, 100 μL of this suspension was evenly applied onto a 1×1 cm^2 carbon paper. After drying, the prepared electrode served as the working electrode for subsequent electrochemical characterization and electrocatalytic CO_2 reduction testing. The loading of all catalysts was maintained at 0.5 $mg\cdot cm^2$.

Electroreduction of CO_2 reaction testing. All electrochemical experiments were conducted on a CHI760e electrochemical workstation using an H-type cell. The anode and cathode

chambers of the cell were separated by a Nafion117 proton exchange membrane, each containing 30 mL of 0.1 M $KHCO_3$ solution as the electrolyte. A conventional three-electrode system was employed, with the external voltage supplied by the electrochemical workstation. Besides the working electrode, a Pt sheet electrode served as the counter electrode, and an Ag/AgCl electrode (with saturated KCl solution) as the reference electrode. During testing, a continuous flow of Ar or CO_2 gas at 20 sccm was maintained.

The potentials measured relative to the Ag/AgCl electrode in this study were converted to values relative to the reversible hydrogen electrode (RHE) using Equation 1. The experimental temperature was 25 °C, with the potential of the saturated Ag/AgCl reference electrode being 0.197 V; the pH of 0.1 M $KHCO_3$ was 6.8.

$$E\ (vs.\ RHE) = E\ (vs.\ Ag/AgCl) + 0.059pH + 0.197 \quad (1)$$

Before the electrocatalytic reaction, Ar or CO_2 gas was continuously introduced into the electrolyte at a flow rate of 20 sccm for half an hour to saturate the solution. The catalyst was then activated by 20 cycles of cyclic voltammetry (CV) at a scan rate of 50 $mV \cdot s^{-1}$ within a potential range of 0.1 to -1.4 V *vs.* RHE.

Linear sweep voltammetry (LSV) is a transient measurement technique that evaluates the relationship between applied potential and current density across electrodes. In current work, the changes in current density and the onset potential of the catalyst under Ar or CO_2 atmospheres were determined using LSV curves. This preliminary assessment of the catalyst's hydrogen evolution reaction (HER) and CO_2 reduction reaction (CO_2ER) activity was conducted within a voltage range of 0.1 to -1.4 V *vs.* RHE, at a scan rate of 5 $mV \cdot s^{-1}$.

The electrochemical active surface area (ECSA) can be calculated based on the double-layer capacitance (C_{dl}) using Equation 2, which is directly proportional to C_{dl}. In 0.1 M $KHCO_3$ electrolyte saturated with Ar, a series of cyclic voltammetry (CV) tests were conducted at various scan rates within the non-Faradaic potential range to measure the double-layer capacitance current. The midpoint current difference $\Delta j/2$ ($\Delta j = j_a - j_c$, where j_a and j_c are the anodic and cathodic current densities, respectively) was plotted against the scan rate. The slope of the linear fit to this plot represents the double-layer capacitance (C_{dl}). The scan rate ranged from 20 $mV \cdot s^{-1}$ to 120 $mV \cdot s^{-1}$.

$$ECSA = R_f \times S = C_{dl}/C_s \quad (2)$$

The roughness factor (Rf) is defined, with S typically representing the geometric area of the carbon paper electrode (S = 1.0 cm^2). C_s denotes the double-layer capacitance of the atomically smooth plane under the same electrolytic conditions.

The Tafel slope is tested to analyze the rate-determining step (RDS) in the reaction, as shown in Equation 3. A Tafel slope near 59 $mV \cdot dec^{-1}$ indicates that the protonation of the excited state CO2* to form the COOH intermediate is the RDS. When the Tafel slope of catalyst approaches 118 $mV \cdot dec^{-1}$, the RDS may involve a single electron transfer to CO_2 to form the excited state CO_2 or the proton-coupled electron transfer to generate the *COOH intermediate. A higher Tafel slope suggests that the RDS could be the adsorption of CO_2 or the desorption of CO. Specific scenarios require computational verification.

$$H = b\log j + a \quad (3)$$

η represents the overpotential (V), j is the partial current density of the target reduction product ($mA \cdot cm^{-2}$), and the fitted value of b is the Tafel slope ($mV \cdot dec^{-1}$).

4. Detection and analysis of products

Gaseous products: The gaseous products generated in this study included C_2H_4, CH_4, CO, and H_2, primarily CO and H_2. These are detected and analyzed using a gas chromatograph (GC). A portion of the collected gaseous products was drawn into the GC using a syringe. The concentrations of H_2 and CO were measured using a thermal conductivity detector (TCD) and a flame ionization detector (FID), respectively. The Faraday efficiency (FE) was calculated according to Equation 4.

$$FE_{product} = Q_{product}/Q_{total} \times 100\% = eFn_{product}/Q_{total} \times 100\% \quad (4)$$

$$n_{gas} = pV/Rt \quad (5)$$

$$n_{liquid} = C_i v \quad (6)$$

$n_{product}$ is the molar (mol) content of the product; e is the number of electrons required per molecule, with CO, H_2, and HCOOH each requiring 2 electrons; F is the Faraday constant (96485 $C \cdot mol^{-1}$); Q_{total} is the total charge passed. For gaseous products, p is 1.01×10^5 Pa, V is the volume of a single chamber electrolytic cell (mL), R is a gas constant 8.314 $J \cdot (mol \cdot K)^{-1}$, and T is temperature of 298.15 K. For liquid products: C_i is the concentration of formate produced ($mol \cdot m^{-1}$), and v is the volume of the electrolyte (mL).

Liquid products: DMSO was used as an internal standard to determine the concentration of HCOOH *via* NMR. After the reaction, 300 μL of reaction electrolyte, 50 μL of deuterium oxide, and 150 μL of 0.2 mM DMSO mixed solution were sequentially added to an NMR tube. The

mixture was sonicated for homogenization to prepare the NMR sample. Quantitative analysis was performed using ^{1}H NMR with water suppression mode. The peak areas were integrated, and the concentration of $HCOO^{-}$ was calculated based on the ratio of the peak areas of the product to the internal standard (S1:S2) according to the standard curve of HCOOH.

5. Reference:

[1] KAWABE Y, ITO Y, HORI Y, et al. 1T/1H-SnS_2 Sheets for Electrochemical CO_2 Reduction to Formate [J]. ACS Nano, 2023, 17(12): 11318-26.

6. Supplementary Figures

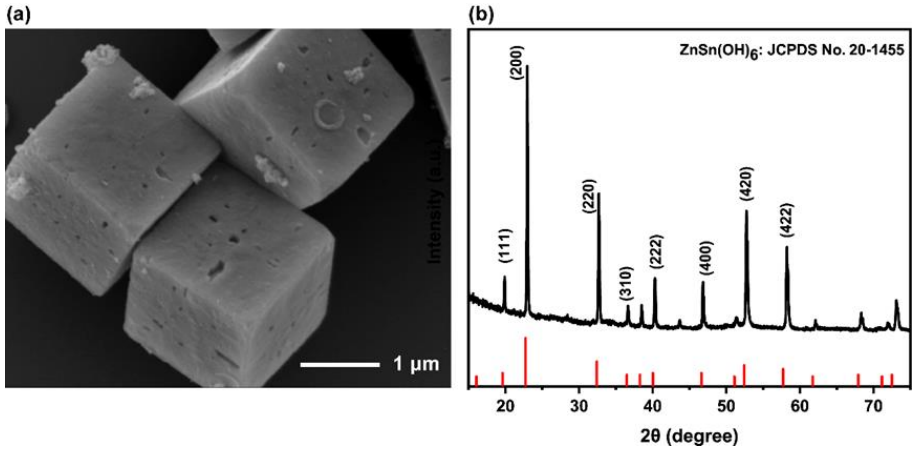

Fig. S1 (a) SEM image and (b) XRD pattern of the $ZnSn(OH)_6$ precursor.

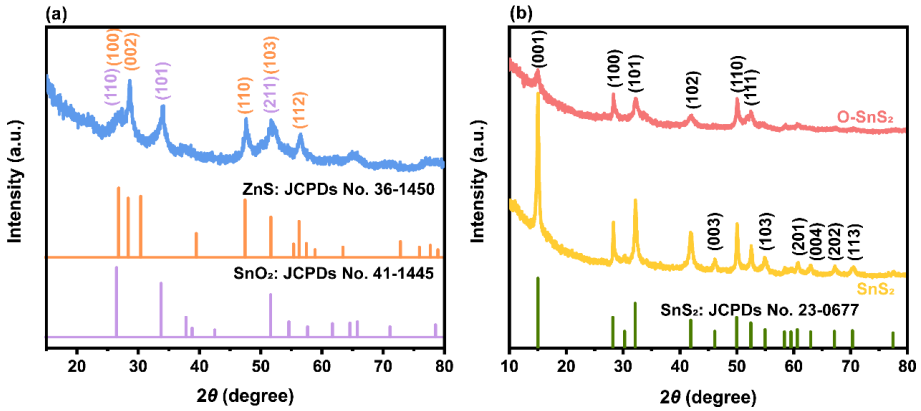

Fig. S2 XRD spectrum of (a) O-ZnS/SnO_2 quadrangular prism, (b) SnS_2 microflower (yellow line) and O-SnS_2 quadrangular prism (red line).

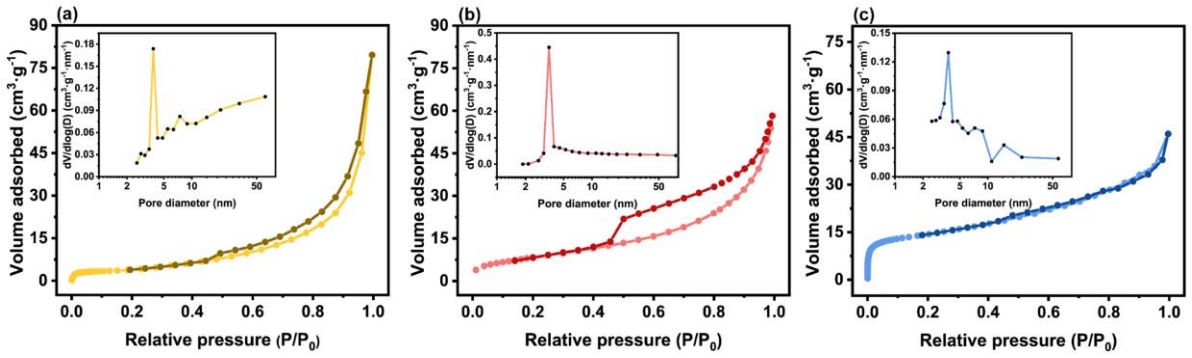

Fig. S3 The N_2 adoption-desorption isotherms and pore distribution (small figures) of (a) SnS_2 microflower, (b) O-SnS_2 and (c) O-ZnS/SnO_2 quadrangular prism.

Table S1 Specific surface area and pore volume of each catalysts

Catalysts	Specific surface area / $m^2 \cdot g^{-1}$	Total pore volume / $cm^3 \cdot g^{-1}$
SnS_2	14.33	0.12
O-SnS_2	32.50	0.09
O-ZnS/SnO_2	50.48	0.07

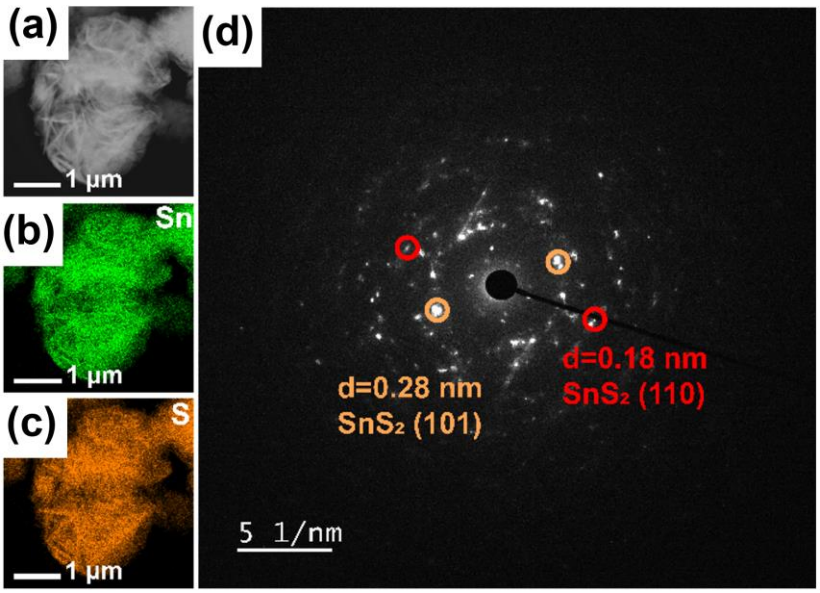

Fig. S4 (a) STEM, EDX spectra elemental mapping of (b) Sn and (c) S, and (d) SAED images of SnS_2 microflower.

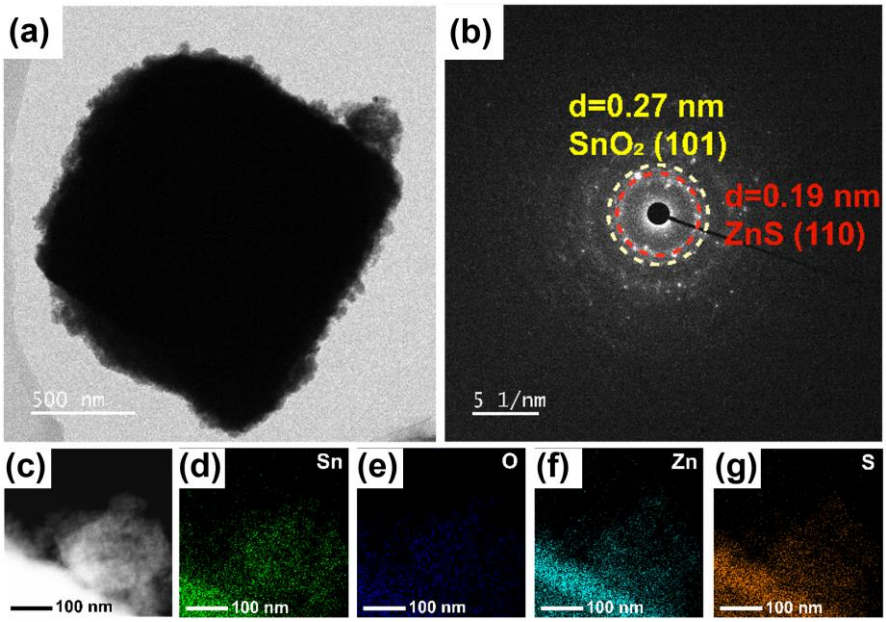

Fig. S5 (a) TEM, (b) SAED, (c) STEM, EDX spectra elemental mapping of (d) Sn, (e) O, (f) Zn and (g) S images of O-ZnS/SnO_2 quadrangular prism.

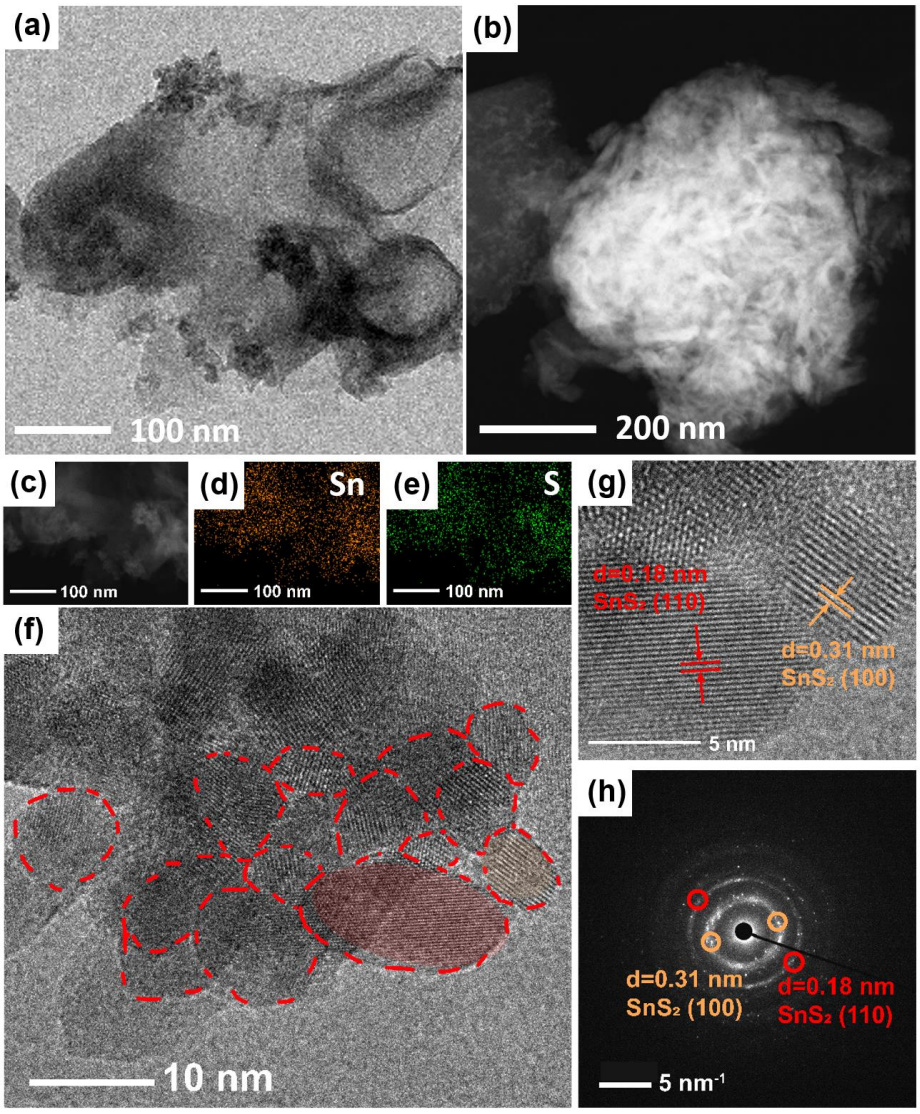

Fig. S6 (a) TEM, (b, c) STEM, EDX spectra elemental mapping of (d) and (e) S, (f, g) HRTEM and (h) SAED images of O-ZnS/SnO_2 quadrangular prism.

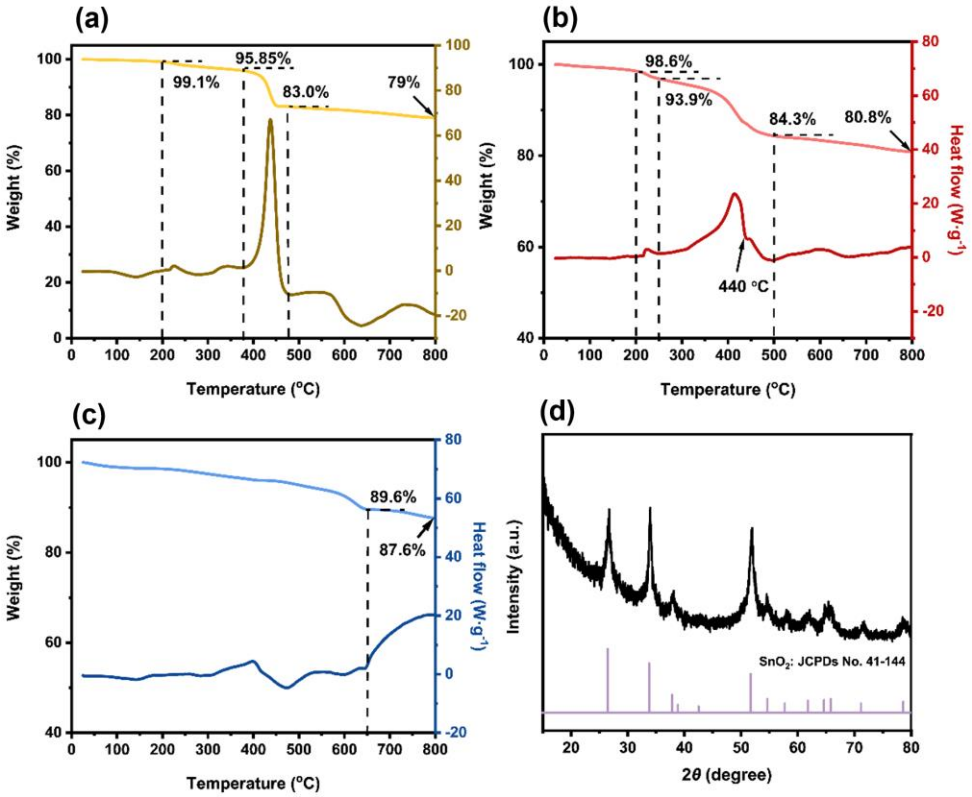

Fig. S7 The TG (top) -DSC (bottom) curves of (a) SnS_2, (b) O-SnS_2 and (c) O-ZnS/SnO_2. (d) XRD pattern of O-SnS_2 catalyst at 440 ℃.

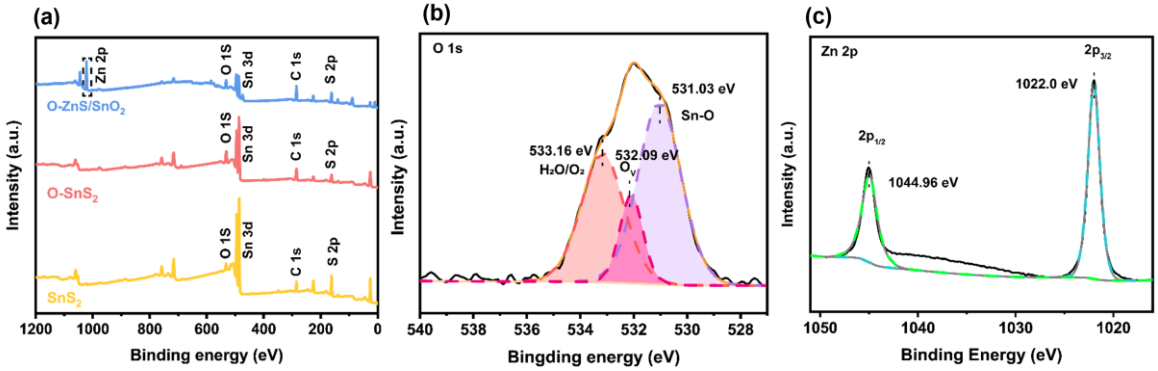

Fig. S8 (a) The XPS Full scan of each catalyst. XPS spectra of (b) O 1s orbit and (c) Zn 2p orbit of O ZnS/SnO_2.

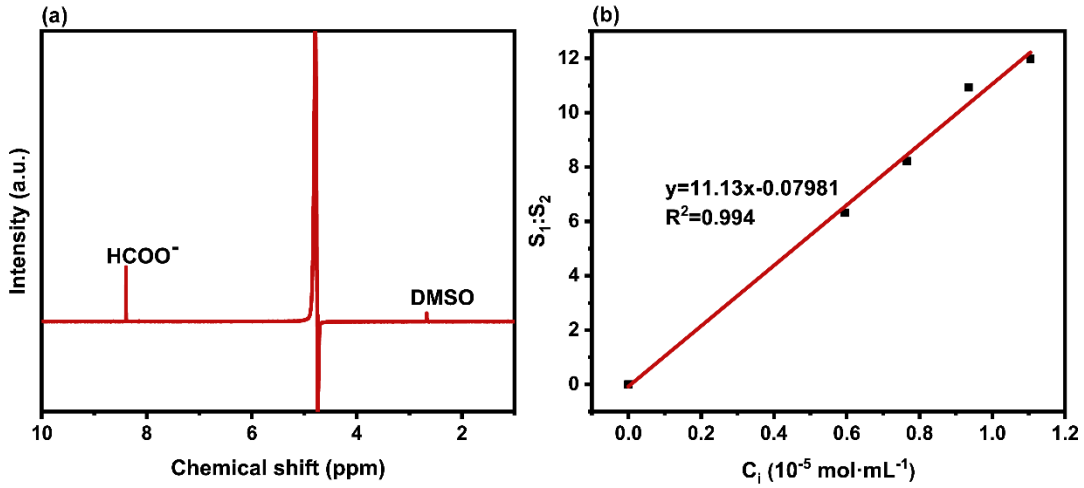

Fig. S9 (a) ^{1}H NMR spectrum. (b) $HCOO^{-}$ standard profile.

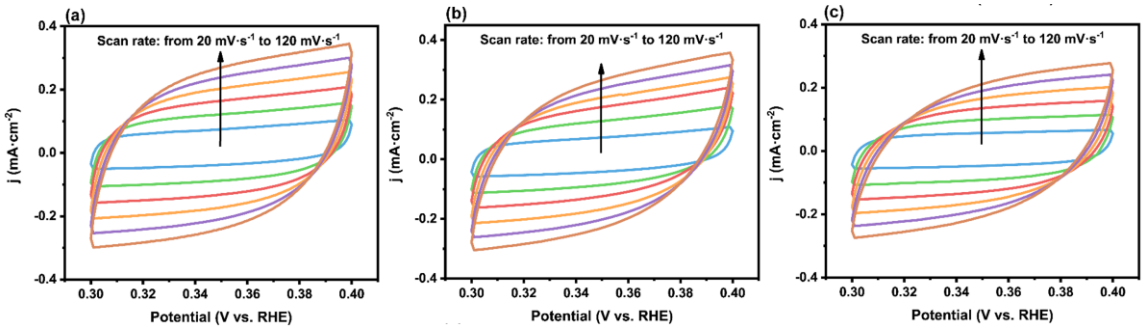

Fig. S10 (a-c) Cyclic voltammetry curves of SnS_2, O-SnS_2 and O-ZnS/SnO_2 at different sweep speeds.